A very-low-cost dosimeter based on the off-the-shelf CD4007 MOSFET array for *in vivo* radiotherapy applications

Authors: O.F. Siebel[(a)], J.G. Pereira[(b)], R.S. Souza[(c)], F.J. Ramirez-Fernandez[(a)], M.C. Schneider[(d)] and C. Galup-Montoro[(d)].

[(a)]School of Engineering of the University of São Paulo, São Paulo, São Paulo State, Brazil, 05508-070.

[(b)]Centro de Pesquisas Oncológicas (CEPON),Florianópolis, Santa Catarina State, Brazil, 88034-000.

[(c)]Instituto Nacional de Câncer (INCA), Rio de Janeiro, Rio de Janeiro State, Brazil, 20230-010.

[(d)]Department of Electrical Engineering of the Federal University of Santa Catarina, Florianopolis, Santa Catarina State, Brazil, 88040-900.

Abstract

Purpose: This paper presents a low-cost MOSFET dosimeter suitable for *in vivo* radiotherapy applications. We analyze different methods to extract the threshold voltage and how this extraction is affected by the dose dependence of slope factor and carrier mobility. Also, we discuss fundamental aspects of the basic building blocks of a MOSFET dosimeter, namely, the radiation sensor, the reader circuit and temperature desensitization.

Methods: Experiments with ionizing radiation (6 MV X-ray beams) were carried out at the Centro de Pesquisas Oncológicas (CEPON) using linear accelerators to test the MOSFET dosimeter.

Results: The main performance parameters of the dosimeter prototype are radiation sensitivity about 100 mV/Gy (sensor's sensitivity is around 6.7mV/Gy), thermal dependence of 0.5 cGy/◦C, reproducibility is about 2.6%, and radiation beam attenuation of 0.14%.

Conclusions: The MOSFET dosimeter described in this article, which combines a simple and accurate readout procedure with a small size, low-cost, cable/battery-free sensor and very little attenuation of the radiation beam is a very appealing option for in vivo dosimetry.

Keywords: MOSFET dosimeter, *in vivo* MOSFET dosimeter, *in vivo* dosimetry, threshold voltage extraction.

I. INTRODUCTION

External radiotherapy is a well-accepted and established therapeutic modality for cancer treatment. In this technique, radiation beams, generated by either linear accelerators (LINAC) or radiation sources, are carefully directed at the patient's malignant tumor with the purpose of delivering a lethal dose to the tumor without inducing significant damage for the patient. The dose precision in radiotherapy is expected to be of the order of ±5%; however, ensuring that the expected dose is properly delivered to the correct spot with the desirable intensity requires a robust and sophisticated radiation oncology Quality Assurance (QA) program [1].

In many cases, due to the complexity of the interactions between the hardware and software, it is virtually impossible to demonstrate with certainty that the operation of the whole system is correct and that all possible failure modes have been eliminated [1]. Consequently, the verification of the final dose delivered to the patient, which can only be carried out by *in vivo* dosimeters, is very important and should in principle be used for all patients undergoing radiation treatments [2],[3]. For the above reasons, we focused our study on the development of a low-cost dosimeter suitable for *in vivo* radiotherapy applications.

The most commonly used *in vivo* dosimeters are based on thermoluminescent, diode and MOSFET devices. TLDs are tissue-equivalent, small, accurate and cable-free. However, the reading procedure represents an important drawback of TLDs because it occurs off-line, it is

time consuming and information is lost during the reading. Although TLD requires a highly trained operator and the cost of the readout equipment is relatively high, it is the most popular dosimeter for QA in radiotherapy [3],[4],[5],[6]. An emerging alternative to TLDs is the Optically Stimulated Luminescence Dosimeter (OSLDs). OSLDs share some characteristics with TLDs (small size and cable-free); however, OSLDs' best practices, *e.g.* to compensate variations in sensitivity and linearity issues, are not yet well established as the TLDs'. On the other hand, the OSLDs' readout procedure, which is (almost) non-destructive, is much simpler and faster than TLDs' [3].

Diode dosimeters provide instantaneous readout; however, diode detectors must be connected to cables during radiation. Even though diode dosimeters are sensitive to the temperature and dependent on the energy of the radiation beam, the correction and calibration factors are generally well known [2],[3],[4],[5],[6].

MOSFET dosimeters are small and capable of storing the accumulated dose; they can be read remotely in a non-destructive way and cables or battery are not required during the radiation application[2],[3],[4],[5],[6],[7]. Considering these characteristics, MOSFET radiation detectors are the most attractive option for clinical in vivo dosimetry; they have features which are impracticable to combine in either TL or diode dosimeters. For instance, MOSFET dosimeters can provide immediate readouts (similar to diodes) and are cable-free (like TLDs). The dependence of the key dosimetric parameter (threshold voltage) on the temperature, which is an important drawback of MOSFETs, can be overcome by the use of differential circuits or choosing a bias current that minimizes the thermal drift [6],[8],[9],[10],[11].

In this article, we begin by recalling the long-term effects of ionizing radiation on MOSFETs. Afterwards, we discuss the main methods to extract the threshold voltage and how this V_T extraction is affected by the dose dependence of the slope factor and carrier mobility. We also present the basic building blocks of a MOSFET dosimeter (radiation sensor, reader circuit and

temperature desensitization). Furthermore, we describe and explain fundamental aspects of the design of the CD4007 MOSFET dosimeter, which is based on the popular off-the-shelf integrated circuit CD4007UBM (Texas Instruments). Finally, we report the results of experiments carried out with ionizing radiation (X-ray beams) performed at the Centro de Pesquisas Oncológicas (CEPON) using LINACs.

II. SUMMARY OF THE EFFECTS OF IONIZING RADIATION ON MOSFETS

Exposure to high-energy ionizing radiation creates electron-hole pairs in the gate oxide of the MOSFET structure. As a result, there is an increase in the charge Q_{ot} trapped in the oxide, mostly near the Si/SiO_2 interface, on exposure to radiation ($\Delta Q_{ot} > 0$) [12],[13],[14],[15].

In addition to the charge trapped in the oxide, ionizing radiation also leads to an increase in the interface traps at the silicon-insulator interface. Interface traps are electrically connected to the semiconductor channel. Consequently, the amount of charge trapped in interface traps is dependent on the biasing conditions [12],[13],[14],[15].

A variation in the total charge in the oxide (oxide-trapped and interface-trapped charges) changes some electrical parameters in MOSFETs [12],[13],[14],[15]. The dominant effect of ionizing radiation on the electrical characteristics of MOSFETs is the shift in the threshold voltage ΔV_T, which is given by:

$$\Delta V_T = -\frac{\Delta Q_{ot}+\Delta Q_{it}}{C_{ox}} \qquad (1)$$

where C_{OX} is the oxide capacitance.

The total charge trapped in the oxide ($\Delta Q_o = \Delta Q_{ot} + \Delta Q_{it}$) is proportional to the oxide thickness (t_{ox}). Since the oxide capacitance decreases with the oxide thickness ($C_{ox} \propto 1/t_{ox}$), as can be observed in (1), the V_T variation due to the ionizing radiation is proportional to ${t_{ox}}^2$.

Thus, MOSFETs with thicker gate oxides have higher radiation sensitivity; however, the supply voltages that have to be employed to detect threshold voltage variations are higher.

In order to illustrate the effect of radiation on the MOSFET, we measured, before and after irradiation, the current-voltage characteristics of PMOS transistors connected as shown in the inset of Figure 1. It is worth noting that the variation in V_T is graphically represented by a horizontal shift ΔV_T in the drain current versus the gate-to-source characteristic of a transistor, as shown in Figure 1 [8],[15]. Note that the threshold variation (horizontal shift) alone cannot fully represent the variation in the I-V characteristic due to ionizing radiation. In addition to the variation in the threshold voltage there is an increase in the slope factor (Δn) [14]:

$$\Delta n = \frac{q\Delta N_{it}}{C_{ox}} \quad (2)$$

where q is the electronic charge ($1.6*10^{-19}$C) and N_{it} is the number of interface traps per unit potential. The increase in n with the dose results in a decrease in the subthreshold slope, as can be observed in Figure 1. In addition to the changes in V_T and n, the carrier mobility μ decreases with the dose [12],[14],[16].

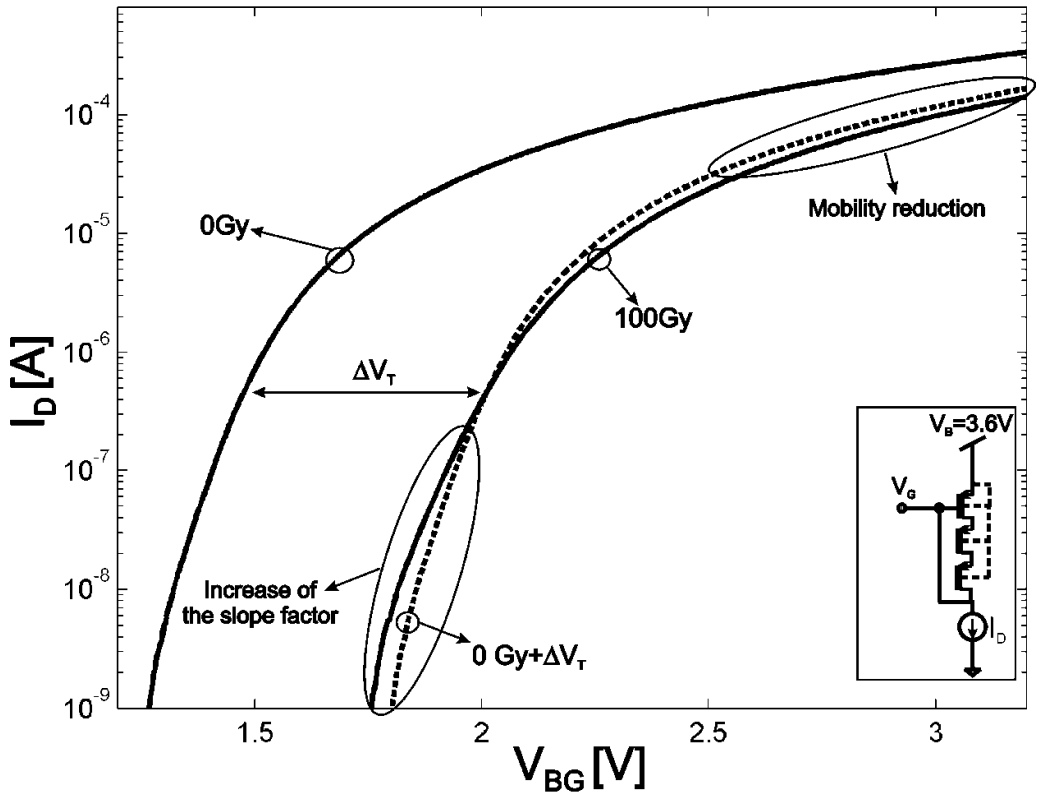

Figure 1. Variation in the current-voltage (I_D x V_{BG}) characteristic (diode connection) for PMOS transistors of the integrated circuit CD4007UBE (Texas Instruments), before and after a 100 Gy irradiation dose (6 MV X-ray). The solid lines were measured for the same transistor before (0 Gy) and after an irradiation dose of 100 Gy. The dashed line is the same curve for the non-irradiated transistor (0 Gy) horizontally shifted by ΔV_T.

III. MESUREMENT OF THE THRESHOLD VOLTAGE SHIFT

The shift in the threshold voltage with the dose is the commonly used dosimetric parameter and two approaches were developed to measure it. In the direct approach [17],[18] the threshold voltage is determined from the intersection of the linearly extrapolated $\sqrt{I_{DSAT}}$ versus V_G curve with the gate voltage axis.

In the indirect method [6], [8],[9], [10], [11],[15],[19],[20],[21], [22],[23] the transistor is biased at a constant current and the gate voltage is measured before and after irradiation. The shift in the gate voltage equals the shift in the threshold voltage if the other parameters of the

transistor (slope factor, mobility, temperature) remain constant during the two measurements. Procedures were developed to compensate for the effect of mobility [11] and temperature [23] variations in the determination of the threshold voltage shift assuming that the transistor follows a quadratic current voltage law (strong inversion model).

The two above-mentioned methods have a common drawback. This relates to the fact that the threshold voltage shift is determined under the hypothesis that the transistor follows a quadratic law, which is only a rough approximation of the current law for large values of V_T-V_G (of the order of several volts). In effect, the threshold voltage is a value for the gate voltage which represents the transition from an exponential regime (weak inversion, WI) to a quadratic regime (strong inversion, SI) [24],[25]. Since this transition is very gradual [24],[25], no specific point can be easily selected and this is one of the reasons why many different threshold voltage extraction methods are described in the literature [17]. Although the extraction methods based solely on the strong inversion model are popular [17], they are inherently inaccurate since they determine the threshold (which is found in between the exponential and quadratic regimes) by extrapolating data from an idealized asymptotic quadratic regime.

Our approach is based on the use of an all-region MOSFET model which allows the direct determination of the threshold voltage and assessment of the error in the determination of the threshold voltage shift at constant current.

In the unified current control model (UICM) [24],[26] the current I_D is written as the difference between the forward (I_F) and reverse (I_R) currents as

$$I_D = I_F - I_R = I_S\left(i_f - i_r\right) \quad (3)$$

where i_f and i_r are the normalized forward and reverse currents, respectively, I_S is the specific current, defined as $I_S = \mu n C_{ox} \frac{\phi_t^2}{2} \frac{W}{L}$, μ is the effective mobility, n is the slope factor, C_{ox} is

the oxide capacitance per unit area, ϕ_t is the thermal voltage and *W/L* is the aspect ratio of the transistor.

For a long-channel PMOS transistor the relation between the applied voltages and the forward current is given by [24],[26]

$$V_S - \frac{V_G - V_T}{n} = \phi_t \left[\sqrt{1 + i_f} - 2 + \ln\left(\sqrt{1 + i_f} - 1 \right) \right] \quad (4)$$

where V_S is the source voltage, V_G is the gate voltage and V_T is the threshold voltage. Voltages are referenced to bulk. Figure 2 shows that (4) is a concise and powerful equation that properly represents (deviations from measurements no greater than 15 mV) the current-voltage characteristics of irradiated MOSFETs over a comprehensive 4-decade current variation ($0.02*i_f$ to $500*i_f$). In this comparison, the gate voltages for irradiated transistors were evaluated taking into account the change of only three electrical parameters (V_T, n, and I_S) as indicated in Figure 2.

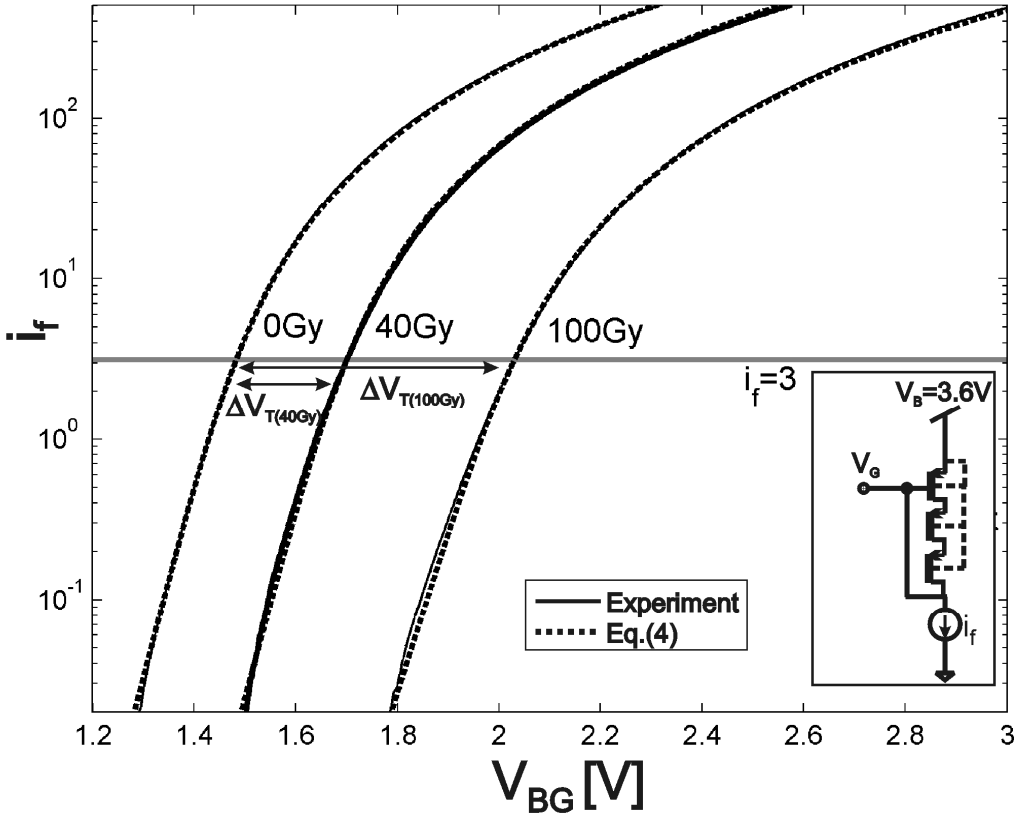

Figure 2. Normalized forward current (i_f) vs. gate-to-bulk voltage (V_{BG}) characteristic for PMOS transistors of the integrated circuit CD4007UBE (Texas Instruments) measured at room temperature (T= 25^{0}C). The solid lines were measured before and after irradiation doses of 40Gy and 100 Gy (6 MV X-ray). The dashed lines are the values from (4), using the following set of MOSFET parameters: $I_{S(0Gy)}$=168 nA, $I_{S(40Gy)}$=173 nA, $I_{S(100Gy)}$=200 nA, $n_{(0Gy)}$=1.35, $n_{(40Gy)}$=1.42, $n_{(100Gy)}$=1.63, $V_{T(0Gy)}$=-1.480 V, $V_{T(40Gy)}$=-1.697V, $V_{T(100Gy)}$ = -2.028 V.

For a transistor operating in saturation (I_F>>I_R) the drain current $I_D \cong I_F$ (the operation of the MOS transistor in saturation is achieved by simply short-circuiting the drain to the gate). Thus, keeping the drain current $I_D \cong I_F$ constant by biasing the MOSFET with a constant current source, and considering that V_S = 0, the relation between the shift in the gate voltage ΔV_G and the shift in the transistor parameters ΔV_T, Δn, and ΔI_S obtained from (4) is

$$\Delta V_T - \Delta V_G = \left(V_T - V_G\right)\frac{\Delta n}{n} - n\phi_t \frac{\sqrt{1+i_f}+1}{2}\frac{\Delta I_S}{I_S} \quad (5)$$

We applied (5), which gives the difference between the gate and threshold voltage shifts (which ideally should be zero), for the selection of an appropriate bias point for the operation of the dosimeter. Firstly, we note that the main parameter for sensing the radiation is the threshold voltage, which changes proportionally to the radiation dose. The other parameters, namely the slope factor and the mobility, are less sensitive to the radiation dose and their variations with the dose are not accurately modeled. The relative variation in the specific current is given by

$$\frac{\Delta I_S}{I_S} = \frac{\Delta n}{n} + \frac{\Delta \mu}{\mu} . \quad (6)$$

In weak inversion (i_f<<1) eq. (5) can be approximated as

$$\Delta V_T - \Delta V_G = \left(V_T - V_G\right)\frac{\Delta n}{n} - n\phi_t \frac{\Delta I_S}{I_S} \quad (7)$$

or, equivalently

$$\Delta V_T - \Delta V_G = \left(V_T - V_G - n\phi_t\right)\frac{\Delta n}{n} - n\phi_t \frac{\Delta \mu}{\mu} . \quad (8)$$

The absolute value of the (negative) threshold voltage of the p-channel transistor increases during irradiation, thus ΔV_T <0. The error due to Δn prevails over that due to $\Delta\mu$ in weak inversion (V_T–V_G < 0), since in this region the slope factor affects exponentially the I-V characteristic (see Fig. 1 and Fig. 2); therefore, for low currents $\Delta V_T - \Delta V_G < 0$ or, equivalently, $\left|\Delta V_T\right| > \left|\Delta V_G\right|$. Thus, in WI the variation in the slope factor makes the measurement of the gate voltage at constant current less sensitive than the direct measurement of the threshold voltage.

In strong inversion (i_f>>1) eq. (5) can be approximated as

$$\Delta V_T - \Delta V_G = \left(\frac{\Delta n}{n} - \frac{\Delta I_S}{2 I_S} \right) \left(V_T - V_G \right) \quad (9)$$

or, using equation (6), as

$$\Delta V_T - \Delta V_G = \frac{1}{2} \left(\frac{\Delta n}{n} - \frac{\Delta \mu}{\mu} \right) \left(V_T - V_G \right) . \quad (10)$$

Since $\Delta\mu<0$ the effects of the slope factor and mobility variations contribute in the same direction and ΔV_T-ΔV_G is at its maximum for the lowest value of the gate voltage (highest value of the current). Since $\Delta V_T - \Delta V_G > 0$, it follows that $\left|\Delta V_T\right| < \left|\Delta V_G\right|$. Thus, in SI the combined variations in the slope factor and the mobility make the measurement of the gate voltage at constant current more sensitive to the dose than the direct measurement of the threshold voltage. However, this increase in sensitivity is due to the variation in the parameters (n and μ) for which the linearity with dose is difficult to evaluate.

Finally, for operation in moderate inversion at i_f =3 (or, equivalently, $V_G = V_T$) (5) reduces to

$$\Delta V_T - \Delta V_G = -\frac{3}{2} n \frac{\Delta I_S}{I_S} \phi_t . \quad (11)$$

Summarizing, the effects of the slope factor and mobility variations are at their maximum deep in weak and strong inversion as it is shown in Figure 3. On the other hand, these effects are expected to cancel at a gate voltage close to the threshold voltage by a value of the order of the thermal voltage.

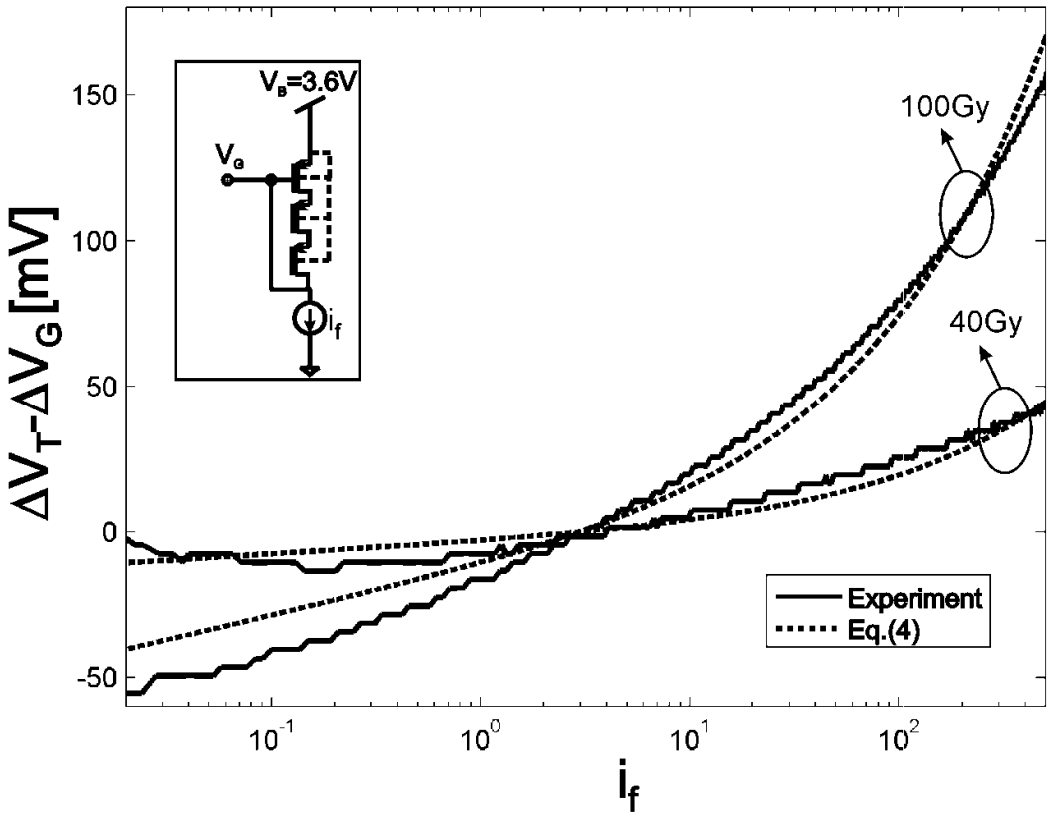

Figure 3. ΔV_T-ΔV_G vs. normalized forward current (i_f) for PMOS transistors of the integrated circuit CD4007UBE (Texas Instruments). The solid lines were measured, before and after irradiation doses of 40 Gy and 100 Gy (6 MV X-ray). The dashed lines use (4) and the values presented in Figure 2. The variation of the threshold voltages ($\Delta V_T = V_{T(irradiated)} - V_{T(0Gy)}$) are -218 mV and -548 mV for doses of 40 Gy and 100 Gy, respectively.

Thus, considering that the sensitivity of the dose to transistor parameters other than the threshold voltage is minimized for operation close to the threshold limit, we decided to bias the transistor with i_f=3 or, equivalently, with I_D=3I_S.

IV. CD4007 MOSFET DOSIMETER

In a MOSFET dosimeter the dose is inferred from the variation in the threshold voltage (or a voltage dependent on V_T). The V_T variation (in mV) measured by a reader circuit is converted into a corresponding dose value (in Gy). During the dose readout, any changes in temperature

must be compensated for, since V_T is dependent on temperature. Finally, the dosimeter processes the data and computes the dose (Figure 4).

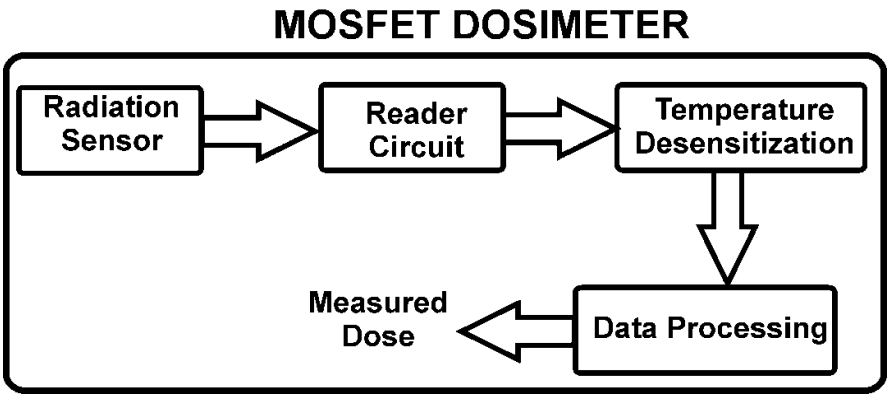

Figure 4. Flowchart of the basic building blocks of a MOSFET dosimeter.

This section discusses fundamental aspects of the design of the basic building blocks of the CD4007 MOSFET dosimeter.

1) Radiation Sensor

The threshold variation is a key parameter for MOSFET dosimeters. A thick gate oxide ($\Delta V_T \propto t_{ox}^2$), usually hundreds of nanometers, is required to provide the radiation sensitivity appropriate for radiotherapy applications [7], [8],[9], [10],[13],[20],[27].

The CD4007 MOSFET dosimeter uses PMOS transistors of the integrated circuit (IC) CD4007UBM as the radiation sensor. This IC was chosen because: (i) a relatively low supply voltage is required to bias the sensor since $|V_T|$ is around 1.6 V, (ii) the gate oxide thickness of the transistors is 120 nm, leading to a radiation sensitivity of around 6.7 mV/Gy, which is convenient for the envisaged application. Also, this IC has small dimensions (area of 38 mm^2 and thickness of 1.75 mm), low-cost (around US$ 0.5) and is cable-free (during irradiation) [7]. Some other dosimeters [8],[21],[28] use batteries to bias the MOSFET sensors to increase their sensitivity, but at the expense of the use of cables.

It is reported in [13] that the CD4007UBE is operational even for an accumulated total dose of 200 Gy, although exposure to extreme doses reduces the average radiation sensitivity to 5 mV/Gy. It is important to note that both the ICs CD4007UBM and CD4007UBE are from the same family, CD4007UB, and differ only in terms of the packaging type: dual-in-line package (E) and small-outline-package (M) [29] and they have basically the same radiation sensitivity [7],[30]. In this study, we chose for the experiments the smaller IC, that is, CD4007UBM.

2) *Reader circuit*

In the most common reading method for MOSFET dosimeters, constant-current (CC) reader circuits are used [6],[8],[9],[10],[11],[15],[19],[20],[21],[22]. A constant-current circuit has a PMOS transistor biased with a constant drain current, as shown in Figure 5.

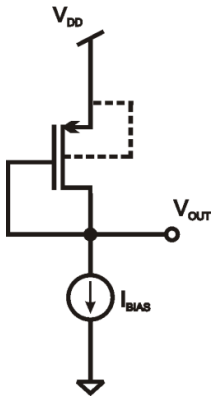

Figure 5. Schematic for the constant-current (CC) reader circuit.

For reasons presented in Section III, arbitrarily selecting the bias current, as employed in [8],[15],[20],[21],[22] is not appropriate for the design of the reader circuit of MOSFET dosimeters. In the CD4007 MOSFET dosimeter that we have developed, the bias current chosen was $3*I_S$ (i_f=3), because with this bias condition we can achieve good sensitivity and linearity with low power consumption (see analysis in the Section III for details). Furthermore, biasing the MOSFET with an inversion level of 3 provides a simple and accurate method to extract the threshold voltage [7],[13],[25].

It is important to note that the dose reading is taken with the MOSFET sensor operating in saturation. Consequently, the transistor is more susceptible to short-channel effects [25]. In order to reduce the short-channel effects and improve the accuracy, the CD4007 MOSFET dosimeter uses a "long-channel" transistor, *i.e.*, three PMOS transistors from the IC CD4007UBM are connected in series, resulting in an equivalent transistor with a channel length three times longer (Figure 6) than that of a single transistor [7].

3) Temperature Desensitization and Data Processing

The threshold voltage of a transistor is strongly dependent on the temperature (for PMOS transistors of the CD4007UBE the thermal coefficient of V_T is around 2mV/°C which represents nearly 0.3Gy/°C [7]). Thus, a temperature variation can be falsely registered by the dosimeter as a dose variation. Consequently, the error originating from temperature variations needs to be minimized. Two approaches are generally used to minimize this dependence: transistor biased at the current (I_{MTC}) for minimum temperature coefficient (MTC) [6],[9],[10],[11],[23] and differential measurements [6],[8],[21].

Biasing the transistor at the minimum temperature coefficient (MTC) current, usually in strong inversion (the MTC current for PMOS transistors of the CD4007UBE is about $375*I_S$ [13]), leads to high power consumption and linearity issues (Section III). In fact, the authors of [11],[23] used multiple bias currents combined with a cumbersome algorithm to improve the linearity of a MOSFET dosimeter biased with the MTC current. Also, it is important to note that the value of the MTC current changes with the dose; therefore, in some cases, it would be necessary to use multiple MTC currents for proper compensation of the temperature variation in a complete treatment [6],[16].

For these reasons, we chose the differential approach, at the expense of an increase in the number of components and the need for matched MOSFETs [7], but without requiring complicated methods to compensate for the thermal or bias dependence of the sensor

parameters. The CD4007 MOSFET dosimeter uses two matched CD4007UBM ICs, one of them as the radiation sensor and the other as the sensor replica (Figure 6).

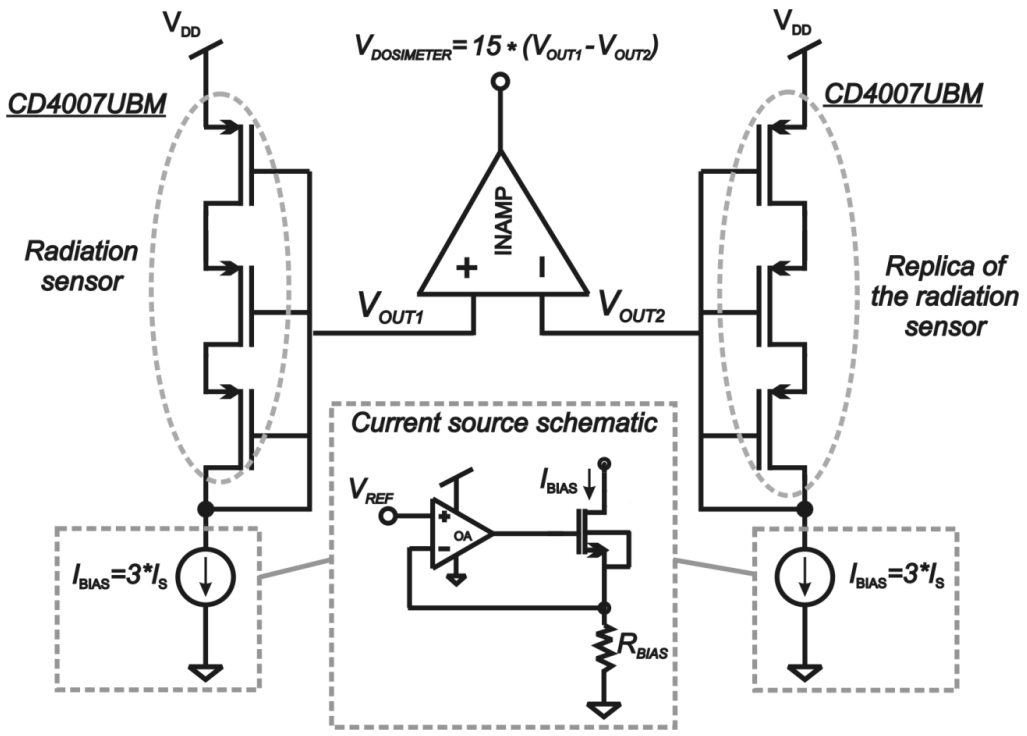

Figure 6. Simplified schematic of the CD4007 MOSFET dosimeter. The maximum input referred offset voltage and input bias current of the operational amplifiers (OPA2277P) of the current sources are 25μV and 1 nA, respectively, while the instrumentation amplifier (INAMP) gain is 15.

In the CD4007 MOSFET dosimeter, only the sensing transistor is exposed to radiation whereas its replica is not. Since during readout both the sensor and its replica are in the same room and, thus, subject to the same temperature, the difference in the output voltages of the devices will be due to radiation only and (almost) independent of temperature [7]. After a radiation session, the dose is computed by an instrumentation amplifier, which outputs a voltage equal to the amplifier gain times the difference V_{OUT1}-V_{OUT2} between the sensor and its replica[30]. A schematic of the current source that generates the bias current for the radiation sensor is shown in Figure 6. To reduce the error in the value of the bias current we used an operational amplifier with low offset voltage and low input bias current as well as high precision resistors.

4) Readout procedure

The CD4007 MOSFET dosimeter readout procedure consists in reading the output voltage ($V_{DOSIMETER}$) immediately before irradiation and reading it again after each irradiation session (Figure 7). The first reading is aimed at compensating for the offset voltage of the dosimeter due to either sensor mismatch and/or that of the instrumentation amplifier. The unbiased (cable-free) MOSFET sensor is exposed to radiation with floating terminals (Figure 7). The readout procedure takes only 1 second and is performed 3-5 minutes after the end of the irradiation session. The complete experimental setup is composed of the MOSFET dosimeter, a digital voltmeter and a personal computer. The computer is used to control the voltmeter and to calculate the dose.

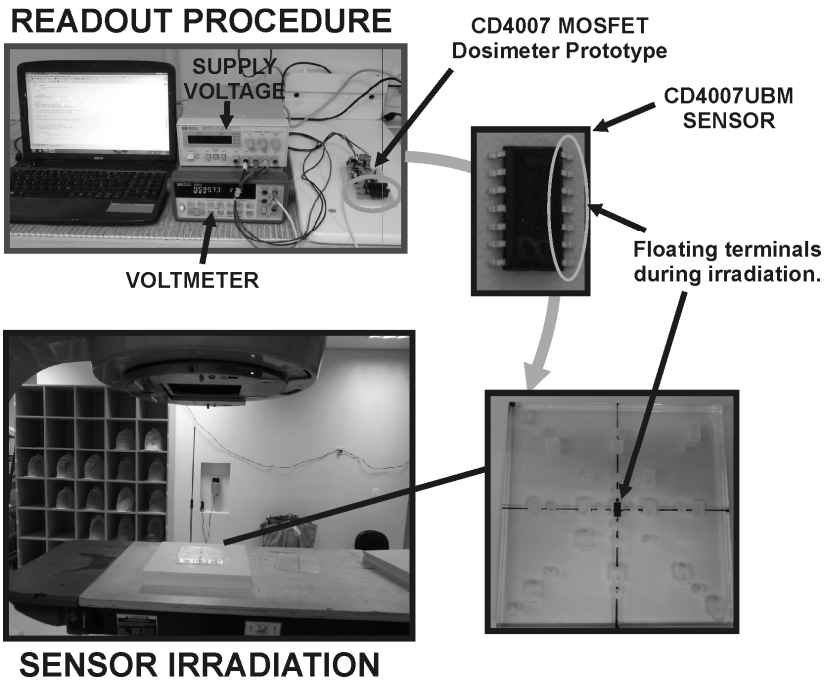

Figure 7. Experimental setup and measurement procedure for the CD4007 MOSFET dosimeter. The output voltage ($V_{DOSIMETER}$) is measured immediately before irradiation; then, the sensor is exposed to the radiation. Finally, the output voltage is measured again after each exposure to ionizing radiation.

It is important to note that each MOSFET sensor can be used multiple times since it remains sensitive to radiation for total doses up to 200 Gy [13].

V. METHODS

This section presents the main characteristics of the experiments carried out to evaluate the performance of the CD4007 MOSFET dosimeter. The sensor was irradiated by 6 MV X-ray beams (field of 10 cm x 10 cm and dose rate of 400 monitor units (MU) per minute) generated by linear accelerators (CLINAC 600C/D and CLINAC 2100C). We used slabs of solid water, acrylic phantoms, an ionization chamber (PTW-TN30013), and thermoluminescent dosimeters (TLD-100, LiF:Mg, Ti). All experiments with ionizing radiation were performed at the Centro de Pesquisas Oncológicas (CEPON).

1) *Temperature Dependence*

The thermal dependence of the MOSFET dosimeter was tested by measuring the output voltage ($V_{DOSIMETER}$) at three different temperatures: 15°C, 25°C, and 35°C. A thermal chamber (Tenney Junior) was used to keep the temperature at the desired value during the experiment for the evaluation of the thermal drift of the dosimeter.

2) *Angular Dependence (Directional Dependence)*

The MOSFET angular response was evaluated through the experimental arrangement shown in Figure 8. In this experiment, one sensor was irradiated with incident angles of 0°, 30°, 60° and 80°. The setup was then rotated horizontally by 90° and the experiment was repeated using another CD4007UBM sensor.

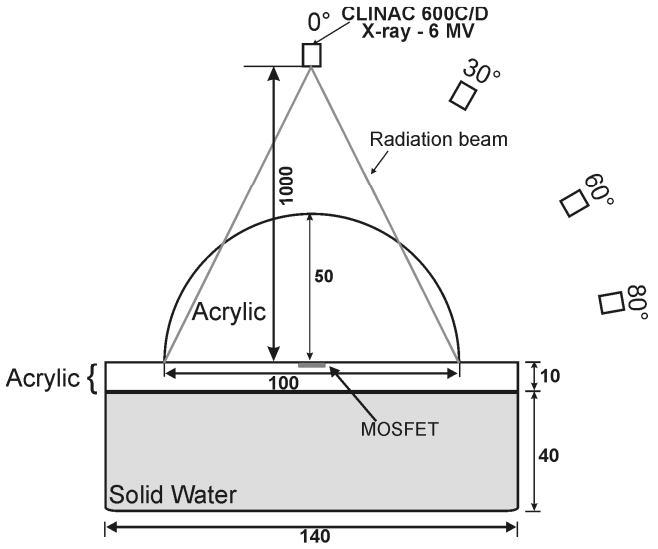

Figure 8. Experimental arrangement used to study the angular response of the CD4007 MOSFET dosimeter (all dimensions in millimeters).

3) Attenuation caused by the MOSFET and TL dosimeters

To evaluate the attenuation caused by the presence of either the CD4007UBM or the TLD (LiF:Mg, Ti, TLD-100) sensor, we used the experimental arrangement shown in Figure 9. In this experiment, an ion chamber was used to measure the variation in the absorbed dose under three different conditions: without both the MOSFET and TLD sensors, with the MOSFET sensor, and with the TLD. In each irradiation session the equipment was set to provide a dose of 2 Gy at the surface of the radiation sensor (MOSFET or TLD).

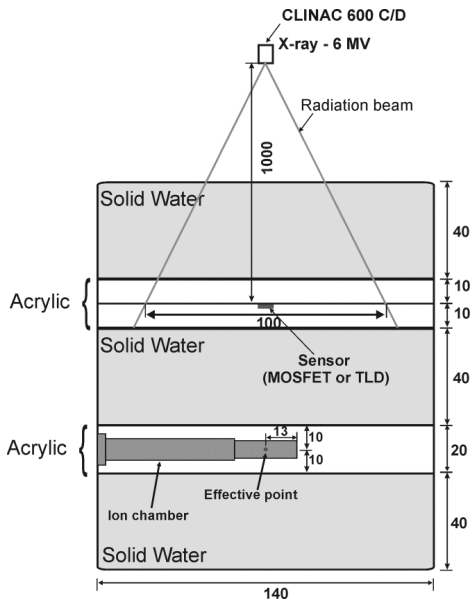

355

Figure 9. Experimental arrangement used to study the linearity and the attenuation associated with the MOSFET and TL dosimeters (all dimensions in millimeters).

4) Dose measurement at multiple locations

The dose at multiple locations was measured using the experimental setup shown in Figure 10.

360 For this experiment, an acrylic slab which allows the placement of 9 MOSFETs and 10 TLDs in a plane of 8 cm x 8 cm (Figure 11) was manufactured.

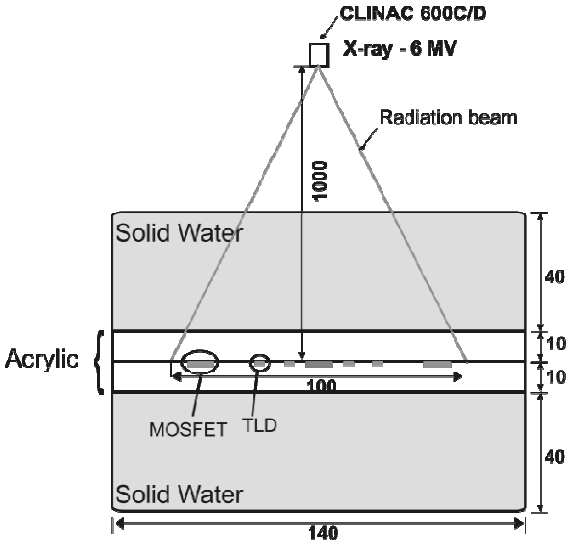

Figure 10. Experimental setup used for the measurement of the spatial dose distribution (all dimensions in millimeters).

Before starting this experiment, a calibration of CD4007UBM sensors was performed. In this calibration procedure thirteen MOSFET sensors were individually placed at the central beam position (Figure 10) and irradiated with 2Gy. In this way, the radiation sensitivity (mV/Gy) of each MOSFET sensor was measured and later used to calculate the dose of each sensor.

Then, 9 calibrated MOSFETs and 10 TLDs were placed at the acrylic slab and received a dose of 2 Gy. After this irradiation session, all TLDs were replaced with another set of TLDs while the MOSFET detectors remained the same. The setup was then rotated by 90°, as indicated in Figure 11. Hence, the dose at each location was measured twice using either a MOSFET or a TLD sensor, except for the positions marked by a dashed circle, which were measured only once with TLDs.

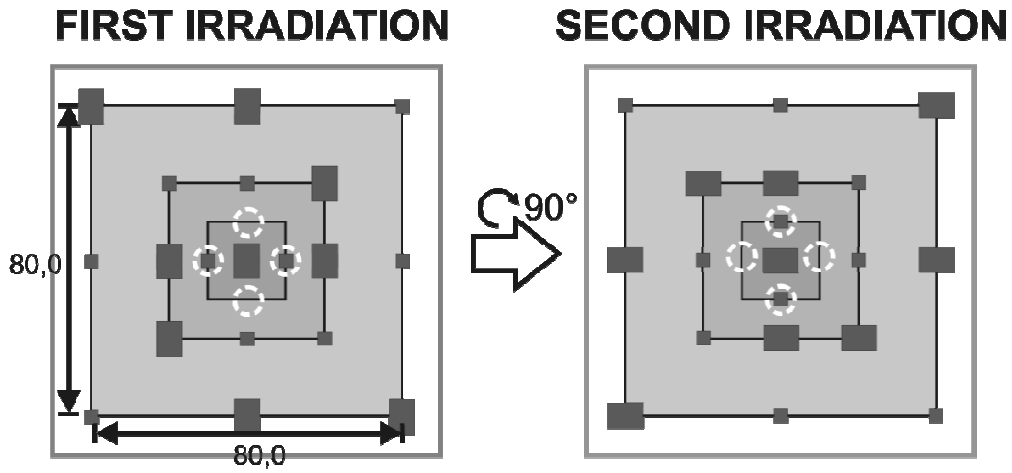

Figure 11. Illustration of the manufactured acrylic slab for the placement of 19 radiation detectors, that is, 9 MOSFETs (large rectangles) and 10 TLDs (small squares). All dimensions are given in millimeters (drawn to scale).

A tomogram of the complete setup was taken and the expected dose at each site was calculated using a treatment planning system (TPS), Eclipse -Varian. All thermal treatment,

calibration, and readout procedures required by the TLD samples were performed in an offsite center, the Instituto Nacional de Câncer (INCA).

VI. EXPERIMENTAL RESULTS

This section presents the results of the experiments with ionizing radiation.

1) *Thermal Dependence*

The dependence of the CD4007 MOSFET dosimeter on temperature is shown in Table I. Only non-irradiated devices were used in this experiment. The thermal sensitivity of the prototype is around 0.5 mV/^{o}C, which roughly translates into an error of 0.5 cGy/°C.

Table I: Variation in the dosimeter output voltage for three different temperatures.

	15°C	**30°C**	**45° C**
$\mathbf{V_{DOSIMETER}}$	-6.1 mV	2.6 mV	10.0 mV

2) *Angular Dependence (Directional Dependence)*

The directional dependence of the CD4007UBM sensor is shown in Table II.

Table II: Dependence of the output voltage on the incident angle of the radiation.

CD4007UBM #63 – Along the major axis				
	0°	**30°**	**60°**	**80°**
$\Delta V_{DOSIMETER}$ (mV)	179	176	166	158
Deviation in relation to the value at 0°	-	-1.7%	-7.3%	-11.7%
CD4007UBM #80 – Along the minor axis				
	0°	**30°**	**60°**	**80°**
$\Delta V_{DOSIMETER}$ (mV)	183	181	168	159
Deviation in relation to value at 0°	-	-1.1%	-8.2%	-13.1%

3) *Attenuation caused by the MOSFET and TL dosimeters*

The variation in the dose measured by the ion chamber due to the presence of MOSFET or TL dosimeters is given in Table III. The deviation in the measurements obtained with the MOSFET or TL sensors is negligible.

Table III. Absorbed dose measured in the ion chamber under three different conditions.

	Ion chamber measurement (cGy)	Deviation with regard to the reference condition (%)
Reference condition (without MOSFET or TL dosimeters)	139.9	-
Using MOSFET	139.7	-0.14
Using TLD	140.0	0.07

400

4) Dose measurement at multiple locations

The result of thirteen CD4007UBE sensors irradiated individually with 2Gy is presented in Table IV.

405 **Table IV.** Radiation sensitivity of thirteen CD4007UBE samples irradiated with 2Gy.

MOSFET #	Radiation Sensitivity (mV/Gy)
37	98.3
62	97.8
58	100.9
54	101.0
45	93.9
102	97.1
66	96.7
105	100.4
87	102.3
72	100.2
86	101.6
24	101.0
78	102.9
Average	99.5
Standard Deviation	2.6

The radiation sensitivity presented in Table IV were used to calculate the dose of each MOSFET sensor given in Table V. The apparatus used for the measurements taken at different sites is that shown in Figures 10 and 11.

Table V. Comparison between the doses calculated by the treatment planning systems and measured with MOSFET and TL dosimeters.

Position (x,y) in cm	TPS (Gy)	MOSFET (Gy)	TLD (Gy)	Deviation 1 (TPS - MOSFET)	Deviation 2 (TPS - TLD)
(-4,-4)	1.95	1.89	1.86	3.08%	4.62%
(-4,0)	1.99	1.99	2.00	0%	-0.50%
(-4,+4)	1.95	1.93	1.88	1.03%	3.59%
(-2,-2)	2.01	2.10	2.00	-4.48%	0.50%
(-2,0)	2.00	2.02	2.03	-1.00%	-1.50%
(-2,+2)	2.01	2.08	2.04	-3.48%	-1.49%
(-1,0)	2.00	-	1.96	-	2.00%
(0,-4)	1.98	2.00	2.04	-1.01%	-3.03%
(0,-2)	2.01	1.99	1.95	1.00%	2.99%
(0,-1)	2.00	-	1.96	-	2.00%
(0,0)	2.00	2.02	-	-1.00%	-
(0,+1)	2.00	-	1.96	-	2.00%
(0,+2)	2.00	2.03	2.02	-1.50%	-1.00%
(0,+4)	1.99	2.03	1.93	-2.01%	2.99%
(+1,0)	2.00	-	2.02	-	-1.00%
(+2,-2)	2.01	2.01	2.07	0.50%	-2.99%
(+2,0)	2.01	2.02	2.02	-0.50%	-0.50%
(+2,+2)	2.01	2.01	1.95	0.00%	2.99%
(+4,-4)	1.94	1.90	1.97	2.06%	-1.55%
(+4,0)	1.99	1.99	1.99	0%	0%
(+4,+4)	1.95	1.93	1.93	1.03%	1.03%
Average	1.989	1.996	1.979	-	-
Standard Deviation	-	-	-	1.87%	2.22%

VII. DISCUSSION

The experimental results show that the CD4007 MOSFET dosimeter has interesting characteristics, offering an average sensitivity around 100 mV/Gy (about 6.7mV/Gy for the MOSFET sensor) and very little attenuation of the radiation beam. The reproducibility for thirteen samples irradiated with 2Gy is around 2.6%, which is comparable with the

reproducibility (1.7%) reported for commercial MOSFET sensors [30],[31]. Also, as reported in [7], radiation sensitivity did not change by more than 2.5% during a 10 Gy irradiation.

The comparison of this MOSFET dosimeter with commercial TLDs, although preliminary, shows that the two dosimeters have similar responses to radiation (standard deviation of around 2%), but the MOSFET dosimeter has advantages over the TL dosimeter, offering a much simpler, low cost and rapid readout procedure. Furthermore, the results for the measurements taken at multiple locations show the possibility of using the developed dosimeter in IMRT applications; therefore, further investigations to evaluate the response of the MOSFET dosimeter using IMRT field patterns need to be conducted.

Comparing our dosimeter with other MOSFET dosimeters (Table VI) we can observe that the sensor used in this work has the lowest radiation sensitivity due to the thinnest gate oxide. The main drawback of lower sensitivity, *i.e.* working with small voltage changes, can be surmounted by a careful electronic circuit design. On the other hand, lower sensitivity usually implies greater lifetime span (maximum dose until saturation) for the MOSFET sensor (the CD4007UBE remains sensitive to radiation up to extreme doses of 200Gy [13]).

Table VI – Important characteristics presented by some MOSFET dosimeters commercially available and/or presented in the literature: **MOSFET** (gate oxide thickness t_{ox}, nominal sensitivity S), **IRRADIATION** (sensor's connection during irradiation), and **TC** (method used to compensate temperature changes).

MOSFET Dosimeter	Important characteristics
This work [7],[13],[30]	**MOSFET** - t_{ox}=120 nm, S=7mV/Gy; **IRRADIATION** - unbiased and cable-free; **TC-** differential measurement.
MobileMOSFET	**MOSFET** –t_{ox}=Not available, S=100mV/Gy;

(Best Medical – former Thomson-Nielsen) [8],[21],[31]	**IRRADIATION** - biased and connected with cables; **TC** - differential measurement.
OneDose (Sicel Technologies)[4],[10]	**MOSFET** – t_{ox}=400 nm; S=100mV/Gy; **IRRADIATION** - unbiased and cable-free; **TC** - MTC current.
MOSkin[28],[32] (Wollongong University)	**MOSFET** – t_{ox}=550nm, S=250 mV/Gy; **IRRADIATION** – Biased and connected with cables; **TC** - MTC current.
Universidad de Granada[11],[23]	**MOSFET** – t_{ox} - Not available, S=30mV/Gy; **IRRADIATION** - Unbiased and cable-free; **TC** - MTC current and multiple biasing.

Also, Table VI shows that the combination of the method used to compensate temperature changes (differential measurement) and the approach used during irradiation (sensor unbiased and cable-free) differentiates this dosimeter from other MOSFET dosimeters. Furthermore, our dosimeter is unique in terms of the design of the reader circuit, particularly, the choice of a bias current in moderate inversion (i_f=3), which reduces the dependence of the dosimeter on MOSFET parameters other than the threshold voltage, a parameter which varies linearly with the radiation doses usually employed in cancer treatment.

It is important to note that although some previous publications, such as [33],[34],[35],[36] have reported experimental results for ionizing radiation using devices of the CD4007 family, to the best of our knowledge this is the first to use the CD4007 integrated circuit as the sensor of a dosimeter for radiotherapy applications [7],[13],[30]. It is interesting to note that some of the authors of [11],[23] that presented the design of a low-cost MOSFET dosimeter using the 3N163 MOSFET transistor, recently changed [37] the MOSFET sensor to the same device

(CD4007UBM) used in this work supporting the appealing characteristics (*e.g.* small size, low-cost, availability, adequate radiation sensitivity) of this device for radiotherapy applications.

The promising results reported in this paper verify the correct operation of the MOSFET dosimeter developed and indicate that further improvements in the prototype should be pursued. In fact, one important characteristic that should be improved is the independence of the measurement on the incident angle. The angular response of a MOSFET dosimeter (with full buildup setup and adequate package) to radiation tends to be uniform in all directions [3],[27]; however, in our prototype the error due to the incident angle of the radiation can be as high as 13%. However, it should be possible to ameliorate this characteristic by using a custom package and reducing the extension of the metal lines inside the standard package shown in Figure 12, where it can be observed that the sensitive area is only a small fraction of the entire package. Consequently, with the design of a custom package not only the extension of the metal lines could be reduced but also the physical dimensions of the radiation sensor.

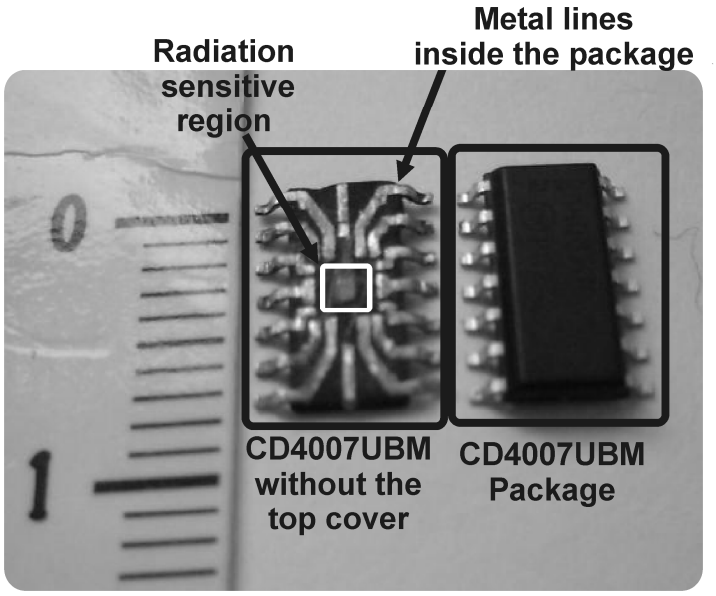

Figure 12. CD4007UBM Small Outline IC (SOIC) package (8.75mm x 4 mm x 1.75 mm) and detail of the metal lines inside the package.

VIII. FINAL COMMENTS

In vivo dosimetry, besides providing verification of the final radiation dose delivered, is a very important technique that should be employed to ensure the efficacy of every radiotherapy treatment, especially those employing the most advanced techniques. Besides accuracy, an ideal *in vivo* dosimeter should have, among others, the following features:

- **transparent to the radiation**, *i.e.*, the dosimeter must be able to measure the dose without interfering or interacting with the treatment beam;
- **comfortable** to help (or at least not compromise) the patient's ability to stay immobile during the treatment, since even a small movement of the patient during the irradiation can be catastrophic;
- **simple and quick readout** is important to promptly detect any error or failure during the dose delivery and to avoid the exposure of subsequent patients to wrong doses. For example, an extreme overdose detected by an *in vivo* thermoluminescent dosimeter that can only be known a few hours after the exposure to radiation and consequently after the treatment of dozens of patients is not the best solution.

The dosimeter presented herein complies with the above requirements. It is cable/battery-free during irradiation and has small dimensions. These characteristics contribute to very low attenuation of the radiation beam, to the patient's comfort, and to rapid setup (no wires need to be passed from the patient to the monitoring unit). Moreover, this dosimeter has a very simple and quick readout procedure which can be easily carried out anywhere by any professional with no need for special skills or training.

In addition to all these features, the CD4007 MOSFET dosimeter is of very-low cost: the radiation sensor (CD4007UBM) costs US$ 0.5 and the prototype can be built for less than US$ 30. The low price of the sensors combined with their reduced dimensions, which aid their storage, allows the use of one (or more) sensor(s) to track the radiation dose given to a patient

throughout the treatment. It is worth mentioning that the cost of an *in vivo* dosimetry system (cost of dosimeters + technicians hours + treatment machine downtime) plays an important role in deciding whether or not this type of dosimetry procedure will be carried out. In fact, reference [3] reports that one factor hindering the widespread use of *in vivo* dosimetry is that there is no general consensus on its cost effectiveness, given that only a small fraction of patients actually benefit from rectifying errors since very few are detected. In this context, the MOSFET dosimeter described in this article is a very appealing option for promoting the use of *in vivo* dosimetry in this context.

ACKNOWLEDGMENTS

The authors would like to thank CNPq and the grant #2013/24894-0 from São Paulo Research Foundation (FAPESP) for the financial support. The help of the Centro de Pesquisas Oncológicas (CEPON), Instituto Nacional de Câncer (INCA), Hospital do Coração (HCor), Daniel Felipe, Eduardo Brandão, and Crystian Saraiva with experimental measurements is greatly appreciated.

REFERENCES

[1**]** J.A. Purdy, E. Klein, S. Vijayakumar, C.A. Perez, and S.H. Levitt, "Quality assurance in radiation oncology" in *Technical Basis of Radiation Therapy: Practical Clinical Applications*, edited by C.A. Perez, S.H. Levitt, J.A. Purdy and S.Vijayakumar (Springer-Verlag, Berlin, 2006), pp 395-422.

[2**]**A.B. Rosenfeld, "Electronic dosimetry in radiation therapy," Radiat. Meas. **41**, S134-S153 (2006).

[3**]**"Development of procedures for in vivo dosimetry in radiotherapy,", International Atomic Energy (IAEA) and International Society for Radiation Oncology, IAEA Human Health Reports, no.8, 2013.

[4**]**A. Jaksic, K. Rodgers, C. Gallagher, and P.J. Hughes, “Use of RADFETs for quality assurance of radiation cancer treatment,” 25th International Conference on Microelectronics, 540-542 (2006).

[5**]**C.J. Tung, L.C. Wang, H.C. Wang, C.C. Lee, T.C. Chao, “In vivo dose verification for photon treatments of head and neck carcinomas using MOSFET dosimeters,” Radiat. Meas. **43**, 870-874 (2008).

[6**]**G. Sarrabayrouse and S. Siskos, "Radiation dose measurement using MOSFETs," IEEE Instrum. Meas. Mag. **1**, 26-34 (1998).

[7**]**O.F. Siebel, J.G. Pereira, M.C. Schneider and C. Galup-Montoro, “A MOSFET dosimeter built on an off-the-shelf component for in vivo radiotherapy applications,” Proceedings of the 5th IEEE Latin American Symposium on Circuits and Systems (LASCAS), 1-4 (2014).

[8**]** M. Soubra, J. Cygler, and G. Mackay, “Evaluation of a dual bias dual metal oxide-silicon semiconductor field effect transistor detector as radiation dosimeter,” Med. Phys. **21**, 567-572 (1994).

[9**]** G. Sarrabayrouse and S. Siskos, Low dose measurement with thick gate oxide MOSFETs, Radiat. Phys. Chem. **81**, 339-344 (2012).

[10**]** P.H. Halvorsen, “Dosimetric evaluation of a new design MOSFET in vivo dosimeter,” Med. Phys. **32**, 110-117 (2005).

[11**]** M.A. Carvajal, M. Vilches, D. Guirado, A. M. Lallena, J. Banqueri, and A.J. Palma, “Readout techniques for linearity and resolution improvements in MOSFET dosimeters,” Sensor and Actuat. A- Phys. **157**, 178-184 (2010).

[12**]** J. R. Schwank, M. R. Shaneyfelt, D. M. Fleetwood, J. A. Felix, P. E. Dodd, P. Paillet, and V. Ferlet-Cavrois, "Radiation effects in MOS oxides," IEEE Trans. Nucl. Sci. **NS-55** , 1833-1853 (2008).

[13**]** O.F. Siebel, M.C. Schneider, and C. Galup-Montoro, "Low power and low voltage VT extractor circuit and MOSFET radiation dosimeter," Proceedings of the 10th IEEE International New Circuits and Systems Conference (NEWCAS), pp.301-304, 2012.

[14**]** R.D. Schrimpf, "Radiation Effects in Microelectronics," in *Radiation effects on embedded systems*, edited by R. Velazco, P. Fouillat, and R. Reis (Springer, Norwell, 2007) pp.11-29.

[15**]** A. Holmes-Siedle, L. Adams, "RADFET: A review of the use of metal-oxide-silicon devices as integrating dosimeters", Radiat. Phys. Chem. **28**, 235-244 (1986).

[16**]** S.H. Carbonetto, M.A.G. Inza, J.L. Lipovetzky, E.G. Redin, L.S. Salomone, and A. Faigón, "Zero temperature coefficient bias in MOS devices. Dependence on interface traps density, application to MOS dosimetry," IEEE Trans. Nucl. Sci. **NS-58**, 3348-3353 (2011).

[17] A. Ortiz-Conde, F. J. García-Sanchez, J. Muci, A. T. Barrios, J. J. Liou, C.-S. Ho, "Revisiting MOSFET threshold voltage extraction methods," Microelectronics Reliability **53**, 90-104 (2013).

[18**]** M. Pejovic, A. Jaksic, G. Ristic, "The behavior of radiation-induced gate-oxide defects in MOSFETs during annealing at 140^{o}C," Journal of Non-Crystalline Solids **240,** 182-189 (1998).

[19**]**G.P. Beyer, G.G. Mann, J.A. Pursley, E.T. Espenhahn, C. Fraisse, D.J. Godfrey, M. Oldham, T.B. Carrea, N. Bolick, and C.W. Scarantino, "An implantable MOSFET dosimeter for the measurement of radiation dose in tissue during cancer therapy," IEEE Sensors J. **8**, 38-51 (2008).

[20**]** A.S. Beddar, M. Salehpour, T.M. Briere, H. Hamidian, M.T. Gillin, "Preliminary evaluation of implantable MOSFET radiation dosimeters", Phys. Med. Biol. **50**, 141-149 (2005).

[21**]** I. Thomson, G.F. Mackay, and M.P. Brown, “Direct reading dosimeter”, United State Patent, US 5,117,113 (1992).

[22**]** Nikola D. Vasović, Goran S. Ristić, “A new microcontroller-based RADFET dosimeter reader”, Radiat. Meas. **47**, 272-276 (2012).

[23**]** M.A. Carvajal, A. Martínez-Olmos, D.P. Morales, J.A. López-Villanueva, A.M. Lallena, and A.J. Palma, “Thermal drift reduction with multiple bias current for MOSFET dosimeters,” Phys. Med. Biol. **56**, 3535-3550 (2011).

[24**]** C. Galup-Montoro and M.C. Schneider, *MOSFET Modeling for Circuit Analysis and Design*, *International Series on Advances in Solid State Electronics and Technology* (World Scientific, Singapore, 2007).

[25**]** O.F. Siebel, M.C. Schneider, and C. Galup-Montoro, “MOSFET threshold voltage: definition, extraction, and some applications,” Microelectr. J. **43**, 329-336 (2012).

[26] A.I.A. Cunha, M.C. Schneider and C. Galup-Montoro, “An MOS transistor model for analog circuit design,” IEEE J. Solid-State Circuits **33,** 1510-1519 (1998).

[27] C.W. Scarantino, D.M. Ruslander, C.J. Rini, G.G. Mann, H.T. Nagle, and R.D. Black, “An implantable radiation dosimeter for use in external beam radiation therapy, ”Med. Phys. **31**, 2658-2671 (2004).

[28] A. Rosenfeld, M.L. Lerch, T. Kron, E. Brauer-Krische, and A. Bravin, “Feasibility study of online high-spatial-resolution MOSFET dosimetry in static and pulsed x-ray radiation fields,” IEEE Trans. Nucl. Sci. **NS-48**, 2061-2068 (2001).

[29] Texas Instruments, “CMOS dual complementary pair plus inverter,” CD4007UB types datasheet (2003).

[30] O.F. Siebel, "Development of an *in vivo* MOSFET dosimeter for radiotherapy applications (in portuguese)," Doctoral thesis, Federal University of Santa Catarina, Santa Catarina, Brazil (2013). Available on line at http://www.bu.ufsc.br/teses/PEEL1560-T.pdf.

[31] Technical Note 1: Dose Reproducibility Assessment (TN#101245.03), Thomson Nielsen Electronic Dosimetry Systems. Available online at http://www.mosfet.ca/global/pdf/technotes/te_1.pdf.

[32**]** Z. Y. Qi, X. W. Deng, S. M. Huang, A. Shiu, M. Lerch, P. Metcalfe, A. Rosenfeld, and T.Kron,"Real-time in vivo dosimetry withMOSFET detectors in serial tomotherapy for head and neck cancer patients," International Journal of Radiation Oncology Biology Physics, pp.1581-1588, vol.50, no.5, 2011.

[33] D.M. Zimmerman and K.P. Ray, "Total dose correlation of 4007 devices flown on the CRRES MEP experiment," IEEE Trans. Nucl. Sci. **NS-41**, 2605-2612 (1994).

[34**]** L.S. August, "Estimating and reducing errors in MOS dosimeters caused by exposure to different radiations," IEEE Trans. Nucl. Sci. **NS-29**, 2000-2003 (1982).

[35**]** S. Rattner and H.E. Boesch, " A comparison of LINAC and ^{60}Co response of the CD4007UBE CMOS inverter," IEEE Trans. Nucl. Sci. **NS-33**, 1051-1052 (1986).

[36**]** P.C. East, "Solid State Dosimeter," United State Patent, US 4,757,202, 1988.

[37**]** M.S. Martínez-García, F. Simancas, A.J. Palma, A.M. Lallena, J. Banqueri, M.A. Carvajal, "General purpose MOSFETs for the dosimetry of electron beams used in intra-operative radiotheraphy," Sensor and Actuat. A- Phys. **210**, 175-181 (2014).